Trans-Eurasian transport of ozone and its precursors

Oliver Wild, Pakpong Pochanart, and Hajime Akimoto
Frontier Research System for Global Change, Yokohama, Japan

Received 30 December 2003; revised 13 March 2004; accepted 14 April 2004; published 2 June 2004.

[1] Long-range transport of air across the European and Asian continents brings substantial quantities of ozone and other oxidants to northeast Asia from upwind sources over Europe and North America. This transport differs significantly from that over the Pacific and Atlantic Oceans because of weaker and less frequent frontal systems over the continent and because of weaker convective lifting over European sources. Slower O_3 formation, faster destruction at low altitudes, and greater deposition over continental regions lead to Europe having a smaller impact on O_3 than other source regions. We present chemical transport model studies of the formation and transport of O_3 from European precursor sources and investigate the extent of their impacts over Eurasia. We focus on measurement sites at 100°E, representing the inflow to east Asia on which regional pollutant sources build, and on northeast Asia, which may be directly affected by transport across Eurasia. The seasonality in O_3 production over Europe is simulated well, and transport principally in the boundary layer propagates these changes in O_3 over Eurasia, leading to monthly mean impacts at Mondy, Siberia, of 0.5–3.5 ppbv. Impacts over Japan are smaller, 0.2–2.5 ppbv, and are very similar to those from North American sources, which dominate at higher altitudes. By following the effect of daily emissions independently, we clearly demonstrate that this greater North American impact is associated with lifting over the Atlantic. European and North American sources contribute to background O_3 over Japan in the anticyclonic conditions that favor regional O_3 buildup and are thus expected to have a small but significant effect on regional air quality. Finally, we demonstrate that location and transport lead to European sources having a different impact on OH, and hence on tropospheric oxidizing capacity and climate, from other major Northern Hemisphere source regions. *INDEX TERMS:* 0345 Atmospheric Composition and Structure: Pollution—urban and regional (0305); 0365 Atmospheric Composition and Structure: Troposphere—composition and chemistry; 0368 Atmospheric Composition and Structure: Troposphere—constituent transport and chemistry; *KEYWORDS:* tropospheric ozone, intercontinental transport

Citation: Wild, O., P. Pochanart, and H. Akimoto (2004), Trans-Eurasian transport of ozone and its precursors, *J. Geophys. Res.*, *109*, D11302, doi:10.1029/2003JD004501.

1. Introduction

[2] Atmospheric oxidants such as ozone formed from precursors emitted over the industrialized regions of the Northern Hemisphere are known to influence air quality over intercontinental scales [*Jacob et al.*, 1999], and may make a substantial contribution to climate change [*Berntsen et al.*, 1996]. The linkage between regional and global environmental impacts is becoming increasingly evident [*Hansen*, 2002], and thus a better understanding of the intercontinental transport of air pollution is required so that policy decisions addressing these issues can be better informed [*Holloway et al.*, 2003].

[3] Transport of pollutants over the Atlantic and Pacific Oceans under favorable meteorological conditions has been clearly identified in coastal observations on western continental margins [*Kritz et al.*, 1990; *Parrish et al.*, 1992; *Jennings et al.*, 1996; *Derwent et al.*, 1998; *Jaffe et al.*, 1999]. These have recently been complemented by satellite observations providing a vivid picture of the evolution of such transport episodes over the oceans [*Husar et al.*, 2001; *Heald et al.*, 2003; *Wenig et al.*, 2003]. Understanding has been advanced by airborne measurement campaigns investigating the export of pollutants from the upwind source regions of North America and east Asia [*Fehsenfeld et al.*, 1996; *Hoell et al.*, 1996; *Jacob et al.*, 2003], and by chemical modelling studies which have demonstrated that this intercontinental transport significantly affects background levels of oxidants at northern midlatitudes [*Berntsen et al.*, 1999; *Li et al.*, 2002], is hemispheric in scale [*Wild and Akimoto*, 2001], and may have substantial impacts on air quality over the continent immediately downwind [*Jacob et al.*, 1999; *Jonson et al.*, 2001].

[4] Transport over Eurasia has received less attention, principally because identification of European impacts over east Asia is more difficult because of additional sources over the continent and different meteorological

0148-0227/04/2003JD004501

factors governing transport. Surface measurements over central Asia show some evidence of impacts from Europe [*Röckmann et al.*, 1999; *Pochanart et al.*, 2003a], but boreal forest fires over Siberia may strongly influence air reaching northeast Asia for much of the year [*Cahoon et al.*, 1994; *Tanimoto et al.*, 2000], obscuring the signature of more remote sources. However, chemical modelling studies suggest that European sources should have a detectable influence on oxidants over east Asia [*Bey et al.*, 2001; *Wild and Akimoto*, 2001; *Liu et al.*, 2002], and that for CO these influences continue to be significant far out over the central and northeastern Pacific [*Staudt et al.*, 2001; *Jaegle et al.*, 2003]. The export of pollution from Europe differs from that from North America or east Asia, where lifting associated with frontal systems plays an important role in export of continental boundary layer pollution over the oceans [*Bey et al.*, 2001; *Cooper et al.*, 2002]. This mechanism is weaker and less frequent over continental Europe [*Stohl*, 2001; *Stohl et al.*, 2002], and consequently a greater proportion of transport occurs in the boundary layer, where transport is slower, chemical lifetimes are shorter, and surface deposition may lead to additional pollutant loss. In addition, outflow from Europe may occur at higher latitudes, where cold temperatures and low insolation suppress chemical formation and surface deposition, and extend lifetimes. While this leads to significant European impacts on the Arctic [*Barrie*, 1986; *Raatz*, 1989], the reduction in chemical processing may give rise to longer-lasting impacts on air quality and climate.

[5] We focus here on two aspects of trans-Eurasian transport: (1) production and export of O_3, CO and NO_y from European sources and the extent of their influence over Eurasia, and (2) the impacts of European sources on east Asia and how they compare with those from North American sources. We examine how the transport of oxidants over the continent differs from that over the Atlantic and Pacific Oceans, and demonstrate that impacts on hemispheric ''background'' abundances of O_3 and CO may contribute to degradation of air quality over the continent. We show that slower chemical processing leads to different effects on tropospheric OH, which controls the lifetime of long-lived greenhouse gases such as CH_4. We describe and evaluate the model and meteorological data used in section 2, and then focus on production and export of oxidants from Europe in section 3. In sections 4 and 5, we quantify the impacts of European and North American sources on CO and O_3 over central and northeastern Asia, demonstrating how vertical transport processes play a large role in defining the long-range impacts of source regions. Finally, in section 6, we examine some of the differences between oxidant export from Europe and that from North America and east Asia, and demonstrate how they may lead to differing effects on climate.

2. Model and Meteorology

[6] This study uses the Frontier Research System for Global Change (FRSGC) version of the University of California, Irvine (UCI), global chemical transport model (CTM), described by *Wild and Prather* [2000]. Two different sets of meteorological data are used to drive the model, allowing the impacts iability in meteorology to be demonstrated. The first is derived from the Goddard Institute for Space Studies (GISS) general circulation model version II′ run at 4° latitude × 5° longitude, with nine levels from the surface to 10 hPa. This data has been used in previous studies of chemistry and transport [*Wild and Prather*, 2000; *Wild and Akimoto*, 2001; *Bian et al.*, 2003]. The second data set was generated with the European Centre for Medium-Range Weather Forecasts (ECMWF) Integrated Forecast System (IFS) at T63 resolution with 19 levels in the vertical, and represents 1996 meteorology. It is used here at T21 resolution (5.6° × 5.6°) as in earlier studies [*Sundet*, 1997; *McLinden et al.*, 2000; *Jonson et al.*, 2001]. Data are supplied at 3-hour intervals in both cases. The key differences between simulations with these data sets are in the treatments of stratospheric chemistry and boundary layer mixing. The linearized O_3 chemistry (Linoz) scheme of *McLinden et al.* [2000] is used to simulate stratospheric O_3 in the ECMWF fields. The vertical resolution in the stratosphere is too coarse for this treatment in the GISS fields, and so the simpler synthetic O_3 (Synoz) scheme [*McLinden et al.*, 2000] is used, with the annual cross-tropopause flux of O_3 set to 550 Tg/yr [*Olsen et al.*, 2001]. In the boundary layer, a simple bulk-mixing is applied every step to simulate turbulence in the ECMWF fields, but the coarser vertical resolution of the GISS fields benefits from a subgrid-scale treatment, and we apply the method of *Louis* [1979].

[7] The annual O_3 budgets from the CTM using these different data sets are presented in Table 1, and illustrate the sensitivity of O_3 chemistry and deposition to meteorological processes. While the net influx of O_3 into the troposphere is very similar, net chemical production and deposition are both lower with the ECMWF fields, despite identical treatments of emissions, chemistry and deposition processes, and similar horizontal resolution. These differences reflect the ways in which turbulent mixing processes, water vapor and surface properties affect oxidant formation, lifetime and deposition.

[8] The distribution of O_3 and its precursors has been compared with long-term surface and ozonesonde observations in previous work [*Wild and Akimoto*, 2001; *Tanimoto et al.*, 2002]. We make further comparisons here to evaluate the model simulations over Eurasia, and to demonstrate the sensitivity to the meteorological fields used. Figure 1 shows the mean annual variations of O_3 and CO at a clean Atlantic coastal site in Ireland (Mace Head, 53°N, 10°W), a mountain site in Germany (Zugspitze, 47°N, 11°E), a remote site in Central Asia (Mondy, 52°N, 101°E) and an elevated site in Japan (Mount Happo, 37°N, 138°E). The site at Zugspitze samples free tropospheric air, but shows a broad summer maximum in O_3, reflecting influence from European emissions. The other sites show the spring maximum and summer minimum characteristic of cleaner, more remote sites in the Northern Hemisphere, although both Mace Head and Happo experience periodic influence from regional pollution sources. The high CO at Happo reflects the strength of regional sources over east Asia. The mean abundance and seasonality is captured well, although there is a tendency to overestimate O_3 in the springtime at low altitudes which is most noticeable at Mace Head. At Mondy, CO is overestimated by 15–30 ppbv, with the largest differences in autumn; this may in part reflect the use of

Table 1. Annual Budget of Tropospheric Ozone[a]

Tendency	GISS II′	ECMWF-IFS
Stratospheric influx	550	519
Chemistry	306	237
Production	3811	4091
Loss	3505	3854
Deposition	855	757
Tropospheric burden	301	283

[a]Fluxes in Tg/yr; burden in Tg.

climatological emissions from boreal forest fires in the model. The variability at the different sites is generally captured well, with relatively small variability at remote sites such as Mondy, and much larger variability at Happo which is strongly dependent on the season.

[9] The use of different meteorological data leads to significant differences in both CO and O_3 at individual sites in some months, but results with both data sets compare reasonably well with the climatological observations. Proximity to major source regions increases the sensitivity to transport patterns and accounts for some of the differences at Mace Head and Happo. However, the systematic differences in springtime CO between the model runs also reflect a differing abundance of OH due to differences in lifting processes, cloud cover and humidity. The mean global lifetime of CH_4 to chemical removal by OH is shorter with the ECMWF fields (9.1 years versus 9.8 years), but differing seasonal and altitudinal distributions lead to slightly greater wintertime buildup of CO. The northward extent of the summertime east Asian monsoonal flow, which brings lower levels of O_3 and CO to Japan, is overestimated with both sets of meteorological data. This reflects the sharp meteorological boundaries over the region that cannot be resolved adequately at the coarse resolutions used here.

[10] To investigate transport over Eurasia in the meteorological fields used here, we calculate the proportion of air masses arriving at the 100°E meridian which may have been exposed to European emissions using the technique of *Newell and Evans* [2000]. Eight-day backward trajectories are calculated from equally spaced points between 20°N and 60°N and between fractions 0.9 and 0.3 of the surface pressure, and the proportion crossing Europe are compared in Figure 2 with those for 1997 meteorology used by *Newell and Evans* [2000]. While we can replicate their results very closely for the conditions and time periods they used, we choose to use longer trajectories to take account of slower transport in late spring and summer, and set them off each day of the year rather than for a 6-day period each month. Over the year we find that 20% of the air masses cross Europe with the GISS fields, 21% with the 1996 fields, and 26% with the 1997 fields, close to the 24% found by *Newell and Evans* [2000], and with a similar range (10–40%). The seasonality is also similar, with a peak in February and minimum in July/August, suggesting that variations in the main flow are reproduced in both sets of meteorological fields, although both show smaller values than with 1997 data in spring and autumn, reflecting higher interannual

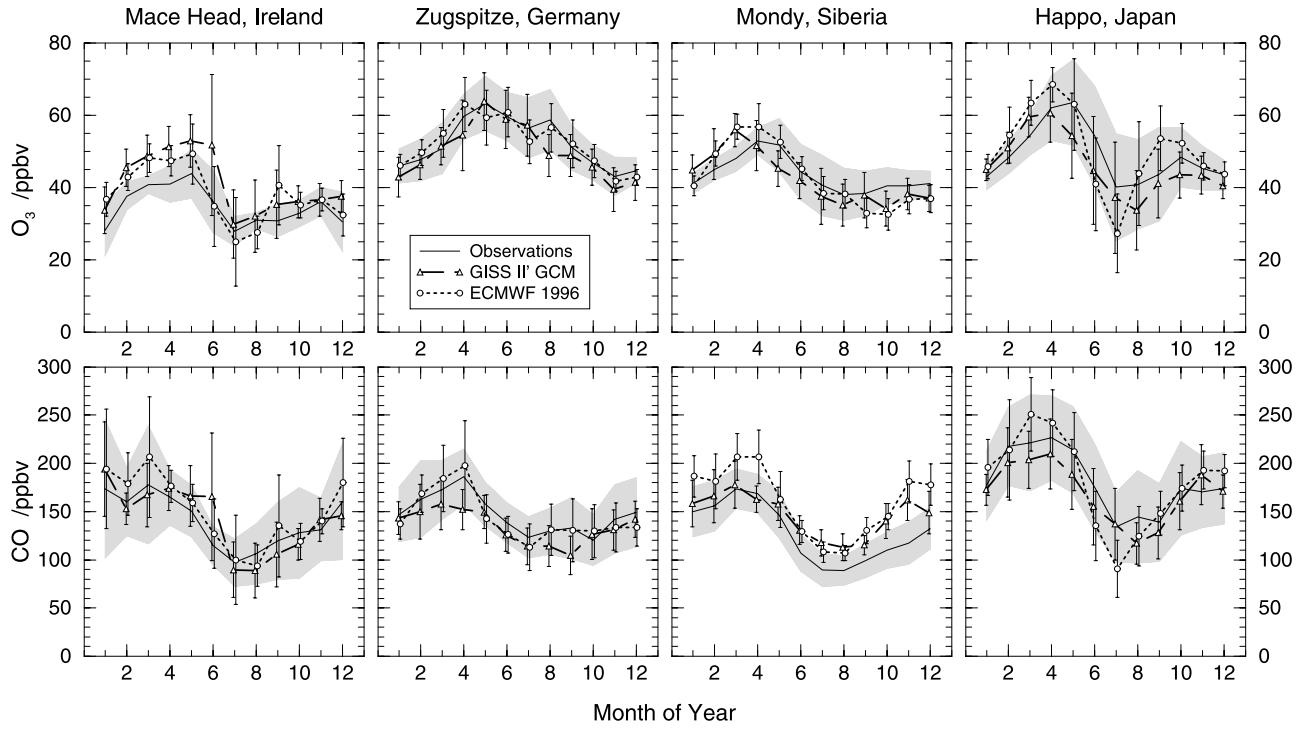

Figure 1. Monthly mean climatology of O_3 and CO at surface measurement sites versus those from the FRSGC/UCI CTM driven by two different sets of meteorological data. One standard deviation in 3-hourly variability about the mean is shown as shading for the observations and error bars for the model results. The sites are Mace Head, Ireland (53°N, 10°W, 25 m) [*Derwent et al.*, 1994], Zugspitze, Germany (47°N, 11°E, 2960 m) [*Graul et al.*, 2003], Mondy, Siberia (52°N, 101°E, 2006 m) [*Pochanart et al.*, 2003a], and H Japan (37°N, 138°E, 1840 m) [*Pochanart et al.*, 2004].

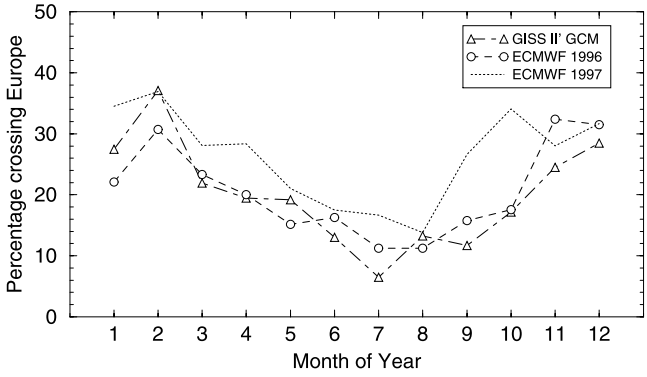

Figure 2. Percentage of 8-day trajectories arriving at 100°E between 20° and 60°N that pass over Europe based on three different sets of meteorology.

variability in these seasons. Despite neglecting convection, chemical transformation, deposition and mixing processes, this analysis provides a valuable indication of the potential of European pollutants to affect Asia, and is of additional interest here as surface measurements of trace gases are available from a number of sites close to the 100°E meridian.

3. European Oxidants

[11] The impacts of industrial and fossil fuel sources on regional and global oxidants are assessed by removing emissions of CO, NO_x, and NMHC over a specified region and comparing the second year of a 2-year simulation with an unperturbed control run. The European region considered here covers approximately 35°–60°N, 5°W–30°E. Studies are performed with both sets of meteorological data and results using the ECMWF fields, with the higher vertical resolution, are presented here unless otherwise specified.

3.1. Ozone Production

[12] Analysis of O_3 observations at continental sites in western Europe using trajectory-based residence time techniques shows a significant contribution from regional sources throughout the year, with a clear maximum in summer, when temperatures and insolation are highest and the timescales for chemical production are thus short. Monthly-mean contributions of 3–20 ppbv were derived from 2 years of surface O_3 measurements at the Swiss alpine site Arosa [*Pochanart et al.*, 2001], while in the lower troposphere, European impacts vary between −4 and 10 ppbv based on 30 years of ozonesonde profiles at Hohenpeissenberg and Payerne [*Naja et al.*, 2003]; see Figure 3. We find similar contributions from European sources with both sets of meteorological data, and a matching seasonality. European contributions are larger in the model in spring and smaller in winter than those derived from trajectory analysis, but the agreement between such widely different analysis techniques, both of which have significant uncertainties associated with them, is very encouraging.

[13] Over northern Europe, where emissions intensities are high and solar zenith angles are larger, summer enhancements are smaller, and $_3$ destruction occurs in winter when direct removal by NO exceeds formation. Observations of O_3 at Norwegian sites show positive contributions from European precursor sources in summer and negative contributions in winter, with the amplitude of this variation larger close to the source regions [*Solberg et al.*, 1997]. We find monthly-mean European impacts that vary between −8 and 10 ppbv over southern Norway (59°N) and decrease to −4 to 6 ppbv at 70°N, in good agreement with this analysis. The annual mean impacts of European precursor emissions on O_3 are 0.7 ppbv and 1.8 ppbv over southern and northern Norway, respectively; interestingly, this is smaller than the mean impacts from North American sources (2.3 ppbv at both sites), although this transatlantic background influence shows a much weaker seasonality, ±0.8 ppbv, with a spring maximum and summer minimum in contrast to the summer maximum and winter minimum of European impacts.

[14] Boundary layer O_3 production from European precursor sources is shown in Figure 4. There is a strong contrast between summer, when regional production is large and net destruction occurs in downwind regions, and winter, when there is net destruction in the region north of 45°N and midlatitude regions downwind experience net production. The regional boundary layer is a net source of O_3 (22 Tg/yr) to the global troposphere, but only accounts for 45% of annual gross production; 23% of production occurs in the boundary layer downwind of Europe and the remaining 32% in the free troposphere. In summer, destruction of exported O_3 exceeds additional formation from exported precursors in the boundary layer east and southeast of Europe, but there is additional formation in northward flow where chemical timescales are longer. In winter, southward outflow leads to significant production over the Mediterranean and North Africa, but northward outflow carries reduced O_3 from northern Europe into the Arctic, where subsequent production is suppressed, and we find that European sources contribute to reduced boundary layer O_3 throughout the Arctic in winter. Interestingly, we find net production from European precursors over the polluted parts of northeast Asia in winter. These regions experience

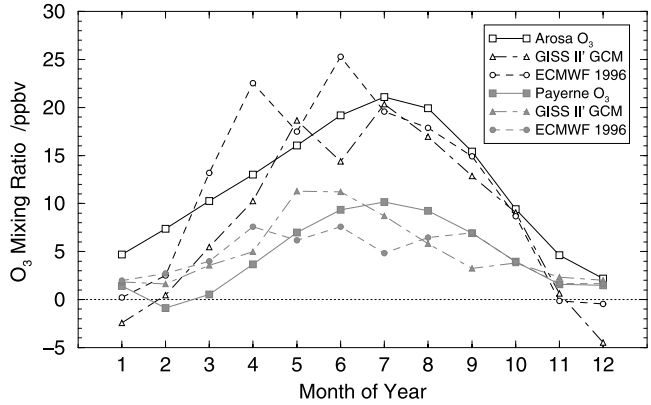

Figure 3. Annual variation in regional O_3 buildup at sites over continental Europe from the CTM compared with those derived from trajectory analysis of surface observations at Arosa [*Pochanart et al.*, 2001] and in the lower troposphere from ozonesondes at Payerne [*Naja et al.*, 2003]. See color version of this figure in the HTML.

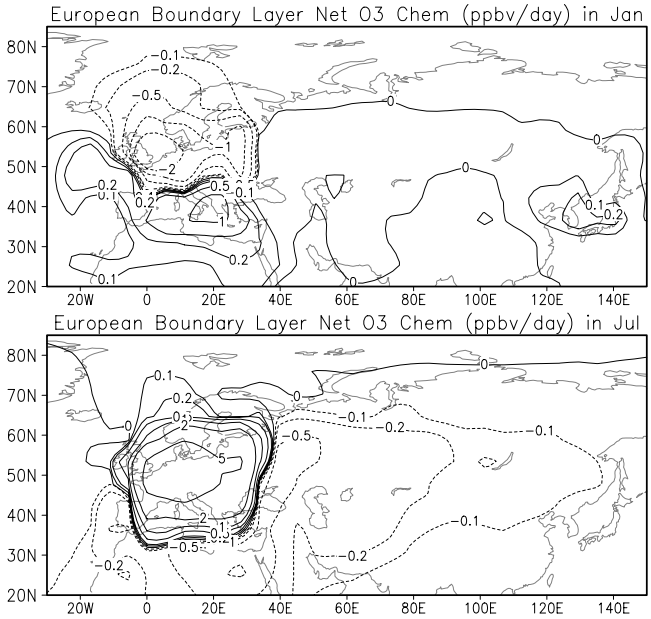

Figure 4. Monthly-mean net O_3 production (ppbv/day) in the boundary layer from fossil fuel sources in Europe in (top) January and (bottom) July.

net destruction in January due to high NO emissions and long chemical timescales [*Zhang et al.*, 2002], and we find that CO and NMHC from European sources are sufficient to reduce this net destruction.

[15] While northern Europe acts as a net sink of O_3 from regional precursor emissions in winter, as analysis of observations has indicated [*Scheel et al.*, 1997; *Derwent et al.*, 1998], it remains a net source of O_3 on a global scale. Removing fossil fuel emissions over northern Europe in January alone, we find net destruction of 0.4 Tg O_3 during the month, but net global production of 2.1 Tg O_3 over the following two months. This highlights the importance of downwind production from exported precursors, which plays a larger role in winter than in summer when timescales for chemical production are short.

3.2. Export of European Oxidants

[16] The fluxes through processes removing O_3, CO, NO_x and NO_y from the European boundary layer are shown in Figure 5. The differing patterns of export reflect the annual cycles in chemical production and loss; O_3 shows a summer maximum, reflecting chemical production, NO_x and NO_y show a winter maximum reflecting longer chemical lifetimes, and CO is relatively constant, dominated by primary emissions. Horizontal advection in the boundary layer is the principal export mechanism for all species, in agreement with earlier studies [*Memmesheimer et al.*, 1997] and in strong contrast to the major source regions of east Asia and North America, where vertical transport dominates [*Wild and Akimoto*, 2001; *Stohl et al.*, 2002]. For O_3, convection and deposition each account for about 20% of removal. Deposition accounts for two thirds of NO_y loss in summer, but only one third in winter when deposition processes are slower and a smaller proportion of NO_y is HNO_3. NO_x makes up only 10% of exported NO_y in summer, but more than half in winter. Convergence and frontal lifting processes peak in winter and spring, but are relatively weak over Europe [*Stohl*, 2001] and make a smaller contribution to total export. Note that the separation of advective and convective processes here is somewhat artificial, and that lifting associated with frontal systems may play a significant role in export due to shallow convection in clouds embedded in the rising air streams [*Purvis et al.*, 2003]. The

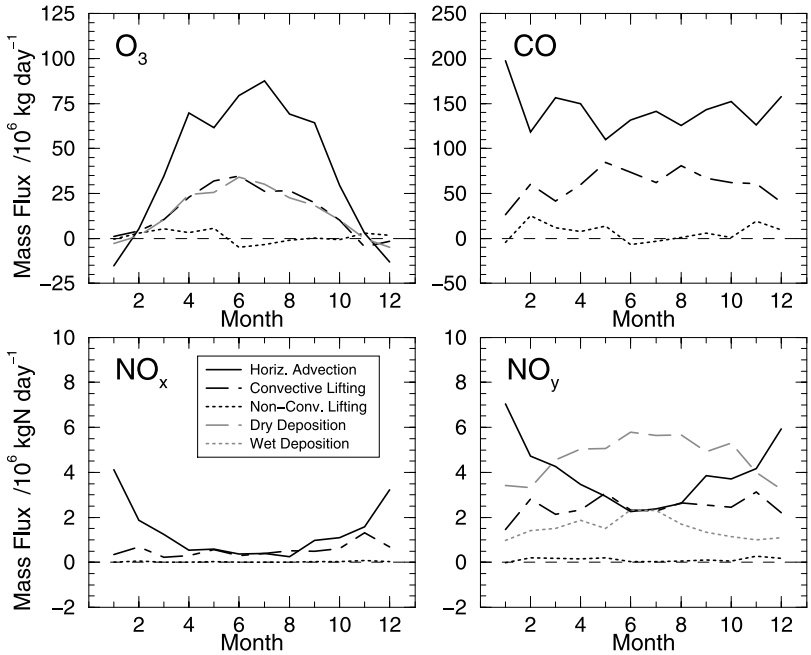

Figure 5. Mass fluxes of O_3, CO, NO_x, and NO_y from European sources through the physical processes controlling removal or export of each species from the continental boundary layer over Europe. See color version of this e in the HTML.

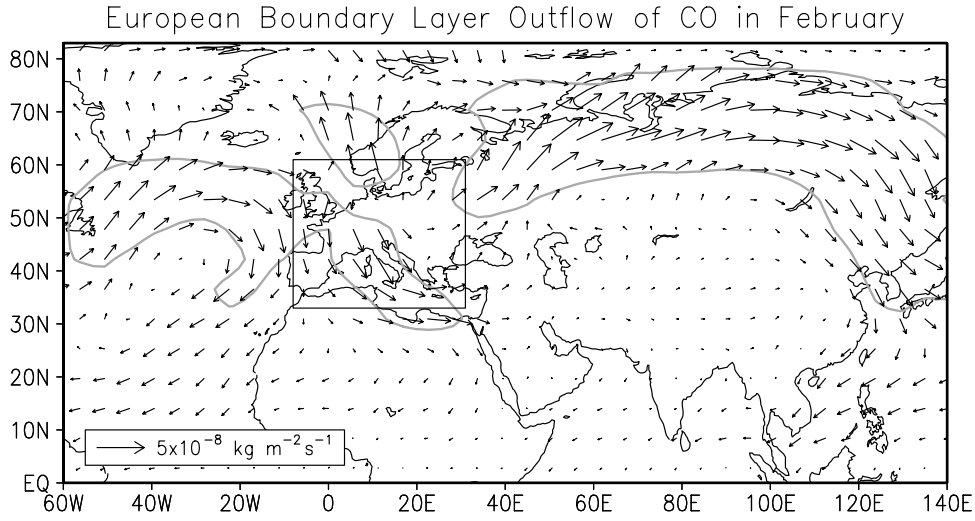

Figure 6. Monthly mean mass fluxes (kg m^{-2} s^{-1}) of CO from European sources in the boundary layer (below 800 hPa) during February revealing the major pathways for export. The grey contour highlights the regions with fluxes greater than 2×10^{-8} kg m^{-2} s^{-1}, and the rectangular box indicates the European emission region considered.

balance of removal processes is found to be similar with the GISS II′ meteorology.

[17] The major pathways for export of European pollution in the boundary layer are shown in Figure 6 for February, when European air has the highest probability of reaching 100°E (see Figure 2). The bulk of outflow occurs in northward and eastward directions, reflecting the effect of high-pressure systems over the continent on the prevailing westerly flow. Anticyclonic conditions over northeastern Europe may lead to direct transport of European pollution into the Arctic [*Barrie*, 1986; *Raatz*, 1989]. The Siberian High established over Eurasia in winter and spring carries European pollution northeastward into the Arctic circle over eastern Russia, and returns it over northeast Asia, where southwestward transport brings European outflow to Korea and Japan. The bulk of this flow crosses Eurasia north of 60°N, suggesting that the trajectory analysis of *Newell and Evans* [2000] may underestimate the potential for Europe to affect east Asia in this season. Subsequent northeastward flow following the storm tracks over the Pacific leads to detectable European influence over the west coast of North America [*Jaegle et al.*, 2003], and circulation around the Pacific High leads to influence over the Equatorial Pacific in spring [*Staudt et al.*, 2001]. In late winter and early spring, flow along the eastern flank of the Siberian High carries European influence southward to Hong Kong [*Liu et al.*, 2002] and into the northeastern monsoon in the tropics, where it may affect southeast Asia [*Pochanart et al.*, 2003b]. We also note here that a significant quantity of CO from European sources encircles the globe at midlatitudes in the middle and upper troposphere. This hemispheric-scale flow is maximum in late winter and early spring when chemical lifetimes are long, and subsidence into the lower troposphere over the North Atlantic leads to this CO reentering the European boundary layer, as clearly visible in Figure 6.

[18] While the principal focus here is on westerly transport over Eurasia, we that southward outflow from Europe occurs for much of the year and leads to impacts on O_3 over the Mediterranean, North Africa, and the Middle East [*Lelieveld et al.*, 2002; *Li et al.*, 2001]. Transport over the Atlantic around the Icelandic Low may lead to direct influence on North America, as noted in previous studies [*Li et al.*, 2002], while southwestward flow around the Bermuda-Azores High leads to influence on the Caribbean [*Hamelin et al.*, 1989]. Some of these pathways for transport of pollution from Europe are described in greater detail by *Duncan and Bey* [2004].

[19] The low altitude of European outflow suggests that there may be substantial impacts on air quality and crop production over populated regions from increased surface ozone and enhanced oxidant deposition. We find annual mean contributions of 2–5 ppbv O_3 over the Middle East, but also note substantial enhancements over Russia north of 45°N, with sources west of 30°E enhancing summertime surface O_3 by more than 3 ppbv as far as 80°E. These impacts are enhanced by the subsidence of air lifted over central Europe and western Russia by frontal systems, and by the mixing of European and Arctic air masses recirculated around high-pressure systems over northeastern Europe in spring.

4. Impacts Over Central Asia

[20] The contribution of European sources to CO and O_3 along the 100°E meridian is shown in Figure 7. The impacts on CO are greatest in the boundary layer in winter and spring at high latitudes, reflecting low-level flow and long lifetimes, and are particularly large in the Arctic in wintertime. Impacts in summer are smaller because of the shorter lifetime, and are larger in the free troposphere than in the boundary layer, highlighting greater vertical mixing and the influence of low-level southeasterly flow. In contrast, the largest impacts on O_3 are in spring and summer when production is faster, and occur in the lower and middle troposphere. Enhancements in the boundary layer are

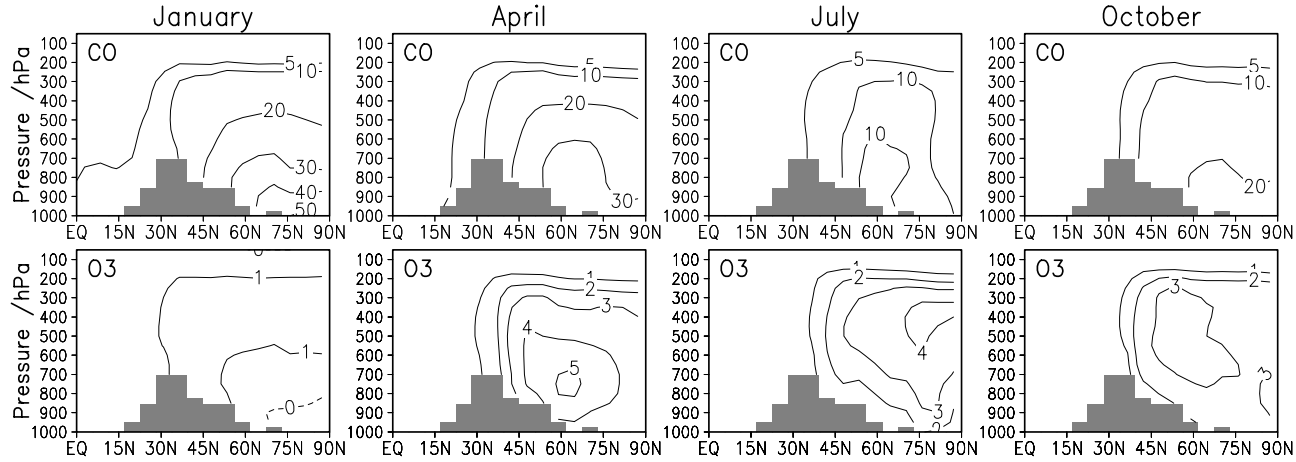

Figure 7. Contribution of European fossil fuel sources (in ppbv) to CO and O_3 along the 100°E meridian. The approximate altitude of topography is shown shaded.

smaller throughout the year because of faster removal. In winter we find reduced O_3 in the Arctic boundary layer, as production and mixing in O_3-depleted air advected from Europe are both slow at high latitudes.

[21] Long-term measurements of CO and O_3 over the central part of Eurasia are available from sites at Mondy, Siberia and Mount Waliguan, China. European contributions at Mondy (52°N, 101°E; see Figure 1) are shown in Figure 8, along with those from North American and east Asian fossil fuel sources. For CO, the mean European influence varies between 30 ppbv in spring and 10 ppbv in summer, with the other regions having a smaller influence but a similar seasonality. For O_3 there is a similar variation between 3.5 ppbv and 0.5 ppbv, although suppressed production over northern Europe in winter leads to a clear, additional minimum in this season. Ozone from North American sources, less affected by these titration processes because of longer, more southerly transport in the free troposphere, dominates during this season. European contributions at Mondy with the GISS II′ fields are similar, 10–28 ppbv for CO and 1.2–3.3 ppbv for O_3.

[22] Observations at Mount Waliguan (36°N, 101°E), 1700 km south of Mondy, show a different seasonality, with a summer maximum in O_3 and a steady decline in CO from a spring peak to a late autumn minimum [*Novelli and Masarie*, 2003]. The European impacts are about 40% of those at Mondy, as the site lies south of the main transport pathways. Fossil fuel sources are responsible for about 50% of the CO at the site but show smaller seasonal variation than at Mondy, largely because of influence from east Asian sources in summer. At Srinakarin, Thailand (14°N, 99°E), farther south along the 100°E meridian, CO and O_3 are greatest during the spring biomass burning season [*Pochanart et al.*, 2003b]. While this site lies in the tropics well away from the main flow over Eurasia, we note significant European influence in winter, reaching 14 ppbv CO and 0.7 ppbv O_3 in February compared with 2–6 ppbv CO and 0.1–0.2 ppbv O_3 at other times of year. However, these enhancements during the northeast monsoon will generally be masked by regional biomass burning influences, making identification from observational data very difficu

[23] Detection of European impacts on CO and O_3 at Central Asian sites relies principally on identification of transport episodes by trajectory analysis. However, over the distances involved here impacts are largely governed by the effects on well-mixed, "background" concentrations. While the signature of transport episodes from Europe can be detected at Mondy [*Pochanart et al.*, 2003a], the full contribution of European sources is not easily quantified. Direct pollutant transport in discrete meteorological episodes is less important for North American than European impacts. This is evident from the smaller temporal variability seen in Figure 8 and is due to greater mixing and

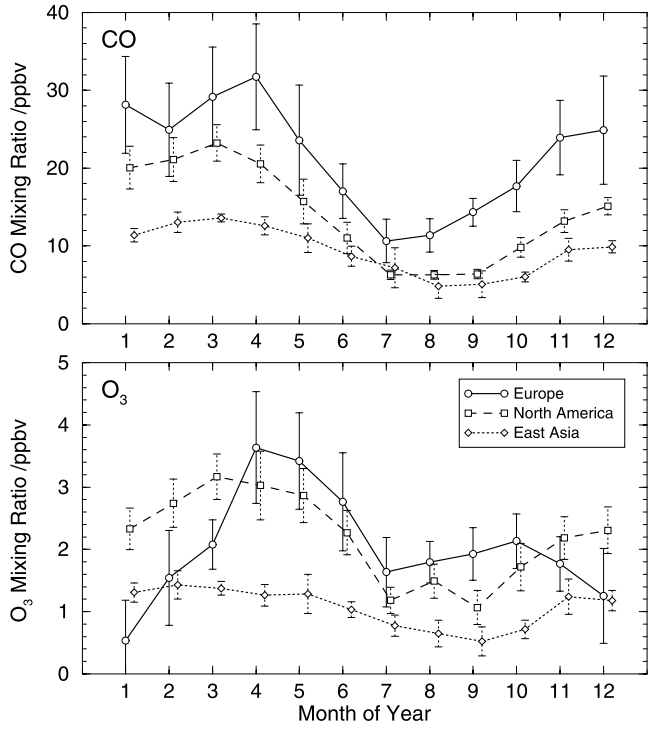

Figure 8. Impacts of northern midlatitude fossil fuel sources on CO and O_3 at Mondy, Siberia. Error bars show 1-σ variability based on 3-hourly data.

chemical destruction over the larger transport distances. To estimate the importance of these episodes, we remove the short-term variability from the 3-hourly data (X) to extract the seasonal cycle (X'), and then calculate the ratio of the mean anomaly ($\overline{|X - X'|}$) each month to the monthly mean ($\overline{X}$). This ratio lies between zero (episodes unimportant) and unity (all transport in episodes). We find annual mean ratios of 0.17 and 0.22 for European impacts on CO and O_3 at Mondy, respectively, and ratios of 0.07 and 0.12 for North American impacts. Episodic transport is more important for O_3 than for CO because of the shorter chemical lifetime and great variability in production, but well-mixed background impacts still clearly dominate. For comparison, we find ratios of 0.19 and 0.23 for North American impacts on CO and O_3 at Mace Head, very similar to European impacts at Mondy, and supporting the conclusions of *Derwent et al.* [1998] that pollutants are generally well dispersed during transport to the site. An alternative measure of episodicity using the ratio of the 90th and 10th percentiles of the monthly distributions presents a similar picture. We conclude that measurements of other more readily attributable tracers will be necessary at these sites if the impacts of particular source regions are to be better constrained by measurements alone.

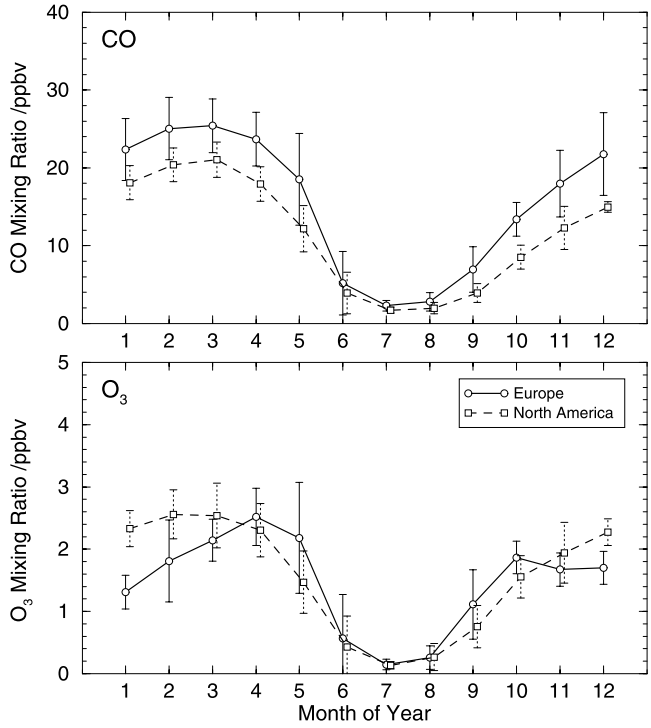

Figure 9. Impacts of northern midlatitude fossil fuel sources on surface CO and O_3 at Happo, Japan. Error bars show 1-σ variability based on 3-hourly data.

5. Impacts on Japan

[24] The southern parts of east Asia are sheltered from pollution transported over Eurasia for much of the year by the Siberian High and by the east Asian summer monsoon. However, most of the air arriving over northeast Asia has been transported over Eurasia, and the impact on oxidants may therefore be substantial. Figures 9 and 10 show the influence of European and North American fossil fuel sources on CO and O_3 over central Japan. Impacts at the surface, 2–25 ppbv for CO and 0.2–2.5 ppbv for O_3, are slightly smaller than those at Mondy, reflecting the greater transport distance, and are much less in summer when the east Asian monsoon flow brings air from the Pacific Ocean. The greatest effects on CO are in the boundary layer, with a maximum in February/March when transport over Eurasia is rapid and the chemical lifetime is longer, and a minimum in July/August. European impacts are about 20% larger than those from North America, in agreement with previous studies of the western Pacific [*Liu et al.*, 2003], and the seasonal patterns are similar. The greatest effects on O_3 appear 1–2 months later (April/May) with a secondary peak in September/October, when the chemical lifetime starts to increase after the summer and stronger zonal flow resumes. Maximum influence occurs in the midtroposphere, in contrast to that of CO and other long-lived tracers, reflecting the greater sensitivity of secondary production and chemical lifetime to altitude. European impacts in the free troposphere are smaller than those from North America, as noted by *Liu et al.* [2002], and occur at a lower altitude, highlighting the different meteorological mechanisms involved. At the surface, we find that European sources have a marginally greater influence except in winter. European contributions with the GISS II′ fields are similar, 3–25 ppbv for CO and 0.3–3.0 ppbv for O_3 at the surface. However, North American impacts are er than European impacts in the free troposphere, largely reflecting weaker lifting over the North Atlantic in these fields.

5.1. Episodes During April 1996

[25] To explore the different effects of European and North American sources on CO and O_3 over Japan in greater detail, we consider the contributions at Happo in April 1996, see Figure 11. During this period the prevailing flow was from the northwest, periodically interrupted by westerly or southwesterly flow associated with frontal systems that bring high levels of pollutants from other parts of east Asia, with major outflow events during 7–8 and 17–18 April. An anticyclone dominated the area between 25 and 28 April, leading to substantial build up of CO and O_3 from local sources over Japan and Korea. European and North American enhancements in CO are very similar in pattern and arrive at the same time, north of the polar front in periods between major frontal systems. The contributions are smaller in the warmer, more humid air arriving with these systems, but the differences are not large, indicating that a well-mixed background influence on CO from these distant sources is present over the whole region. The highest surface CO over Japan occurs during this southwesterly flow and is largely dominated by east Asian sources outside Japan. The factors governing O_3 are notably different. Maximum enhancements from European and North American sources are in the midtroposphere and occur at different times because of the different chemical histories of these air masses and the different transport mechanisms close to the source regions which govern them. Enhancements are much smaller during warm sector flow, indicating that hemispheric background O_3 is less affected by these sources

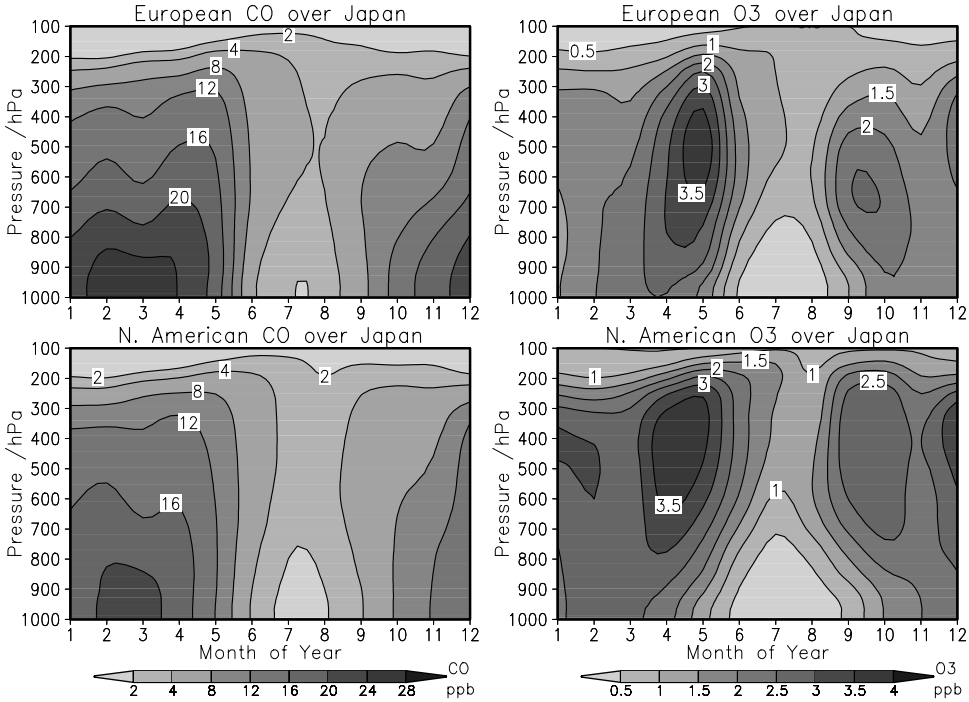

Figure 10. Impacts of European and North American fossil fuel sources on monthly-mean (left) CO and (right) O_3 over Happo, Japan.

than background CO. The highest surface O_3 occurs during anticyclonic conditions and is dominated by local sources, in contrast to CO.

[26] The mechanisms leading to these different O_3 responses are investigated by running 1-day pulses of emissions from North American and European sources for March and April, and examining the evolution of O_3 production and the pathways for transport. Figure 12 shows examples of the altitudinal evolution of O_3 over the Northern Hemisphere north of 23°N from sources over each region. O_3 enhancements are initially high in the regional boundary layer, where 60% of the gross production from North American sources occurs, and 70% from European sources. However, convection and frontal lifting over the western Atlantic raise North American outflow while chemical loss reduces surface O_3, and maximum enhancements after a week occur at 400–500 hPa (5–6 km). Lifting of European sources is weaker, and maximum enhancements remain close to the surface (below 2 km); one week after the emissions, only 38% of the O_3 formed lies above 730 hPa, compared with 62% from North American sources. The general pattern of outflow is similar for different days, although total O_3 production and the strength and timing of lifting vary. In particular, we note that the passage of cyclonic systems over the east coast of North America leads to periodic O_3 buildup in the polluted boundary layer followed by lifting of O_3 from a number of days together, causing significant episodes of outflow, despite little variation in the daily gross regional production (only 8%). Similar lifting occurs over Europe or downwind over western Russia, but maximum enhancements are typically below 600 hPa (4 km), and impacts on the midtroposphere are one third to a half those of Nor erican sources.

[27] The episodic nature of European and North American influence on Japan seen in Figure 11 is dependent on variations in east Asian regional meteorology as well as on variability in outflow from source regions. Back trajectory analysis of the largest North American O_3 enhancement (at 350 hPa on 14 April) reveals the influence of rapid, high-level flow over Eurasia following strong lifting over the western Atlantic, while peak European enhancements (at 800 hPa on 24 April) accompany subsidence from 500 hPa in an anticyclone, preceded by slower, rising flow originating from Europe. CO is also enhanced during these episodes, but the longer lifetime of CO near the surface leads to a smaller contrast than for O_3, and thus they appear less distinct.

[28] By following the O_3 contribution from each day of emissions from North American sources separately, we find that the 14 April episode at 350 hPa is influenced by emissions over an extended period, with the largest impacts from emissions 14 days earlier. However, emissions between 27 March and 2 April only account for 36% of North American O_3 during the episode, demonstrating the importance of a well-mixed background from earlier emissions. Enhanced production in the North American boundary layer between 29 and 31 March followed by efficient lifting to 5–8 km over the Atlantic between 2 and 3 April by a single cyclonic system transports O_3 from 4–5 days emissions together. A second, broader peak at 600 hPa on the same day arises from slower transport at lower altitudes over about 20 days, and results from O_3 from earlier emissions lifted to only 3–4 km over the Atlantic. Analysis of the European contributions to the episode on 24 April shows that O_3 at 600 hPa is dominated by emissions 7 days earlier, but that the largest contributions arrive at 750 hPa after 13 days, reflecting the dominance of slow, low-level trans-

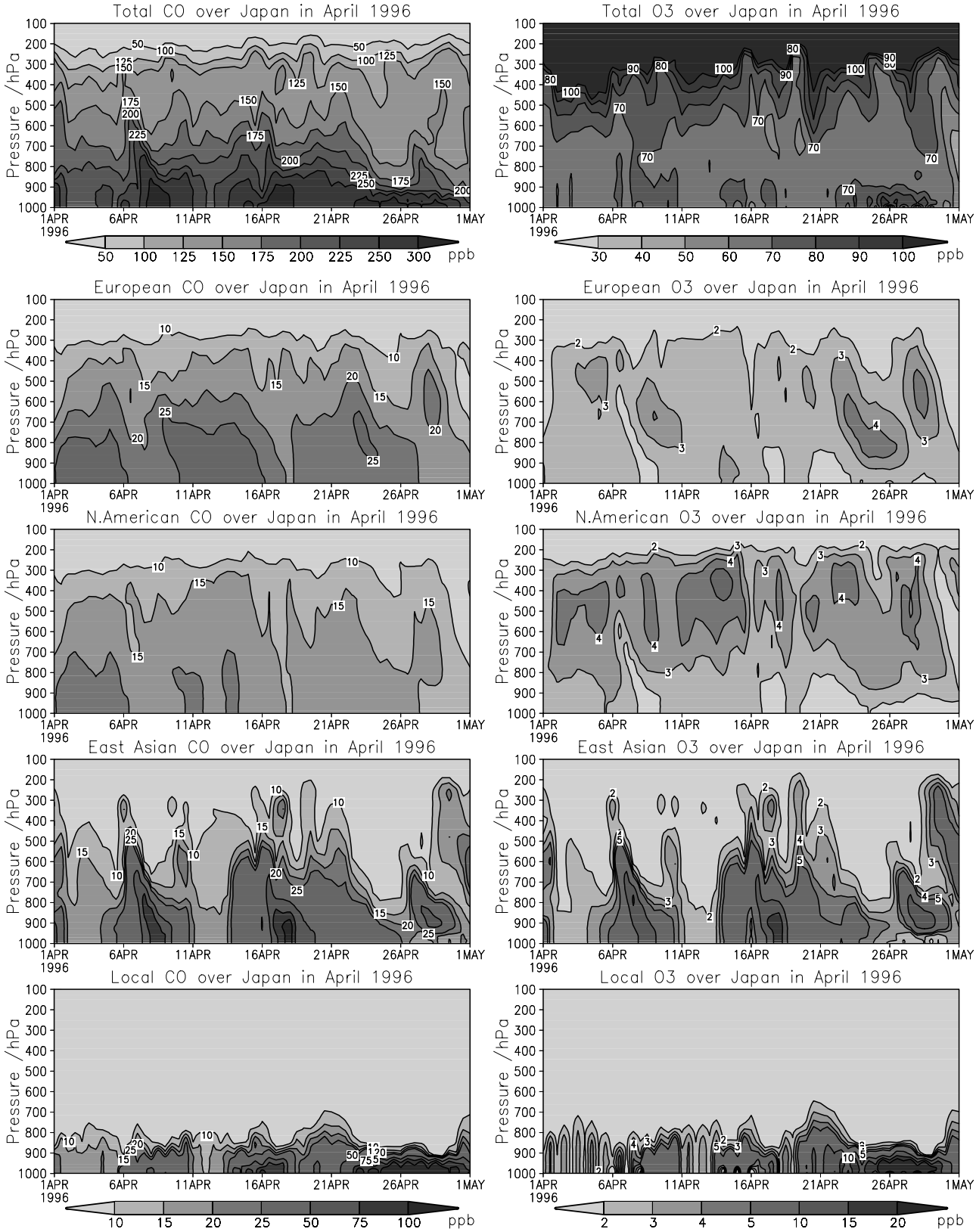

Figure 11. Evolution of the profiles of (left) CO and (right) O_3 over Happo, Japan, in April 1996, together with contributions from European, North American, regional east Asian, and local Japanese fossil fuel sources. See color version of this figure at back of this issue.

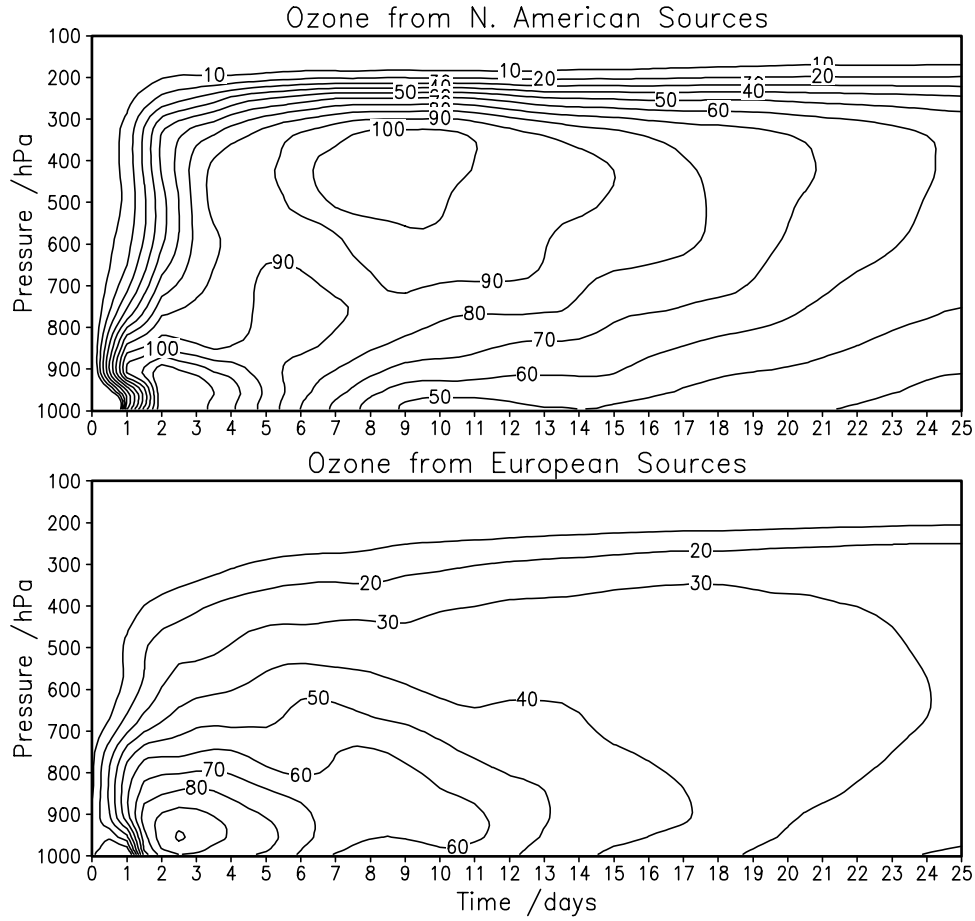

Figure 12. Time evolution of the mean impacts on the Northern Hemisphere extratropical O_3 profile in April (in pptv) from a single day of emissions from fossil fuel sources (top) over North America and (bottom) over Europe.

port. Interestingly, maximum European impacts take almost as long to arrive over Japan as those from North America.

5.2. Air Quality

[29] To what extent do these intercontinental impacts affect air quality over Japan? In summer, when photochemical production of O_3 is fastest, the east Asian monsoon flow brings clean air from the Pacific, and the background concentrations on which urban pollution builds are thus small. The greatest impacts from sources outside Japan occur in late spring, when the buildup of smog O_3 is less efficient, and sources from other parts of east Asia dominate.

[30] Figure 13 shows the variation in O_3 at Happo in April and the contributions from local (Japanese), regional (east Asian) and distant fossil fuel sources. During the first 3 weeks O_3 is overestimated in the model by about 10 ppbv compared with observations. This may be due to the coarse resolution of the model and close proximity to source regions, but is similar to previous springtime comparisons at this site [*Carmichael et al.*, 1998]. Nevertheless, the daily variability and trends over the period are accurately captured. The large buildup of O_3 from local sources during the anticyclonic period in the final week of April is captured rather better.

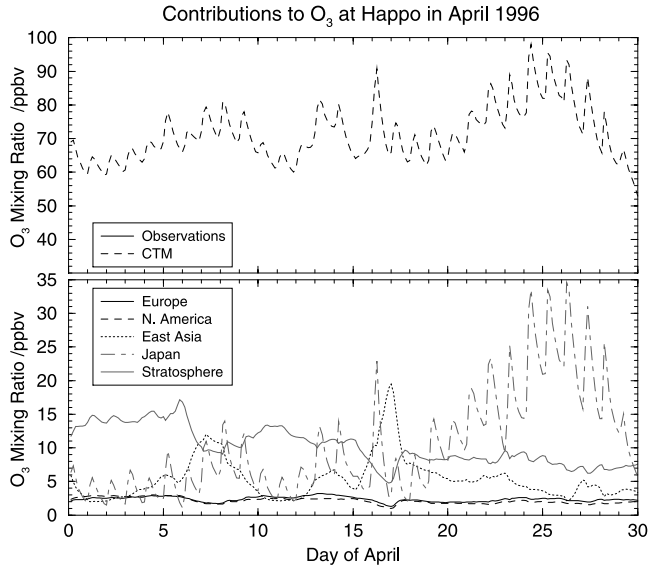

Figure 13. (top) Ozone at Happo, Japan, in April 1996, together with (bottom) contributions from local, regional, and distant fossil fuel sources and stratospheric influx in the CTM. See color version of this figure in the HTML.

Table 2. Annual Mean O_3 Budgets From Regional Fossil Fuel Emissions

Region	Domain	Emissions		Gross O_3 Production			Fraction Deposited	Production Efficiency
		NO_x	CO	Total	>730 hPa	<280 hPa		
Europe	33°–61°N, 8°W to 30°E	4.6 TgN	75 Tg	108 Tg	68%	5%	17%	6.8
North America	22°–66°N, 127°–60°W	7.6 TgN	95 Tg	177 Tg	61%	8%	14%	6.8
East Asia	17°–44°N, 98°–143°E	3.8 TgN	95 Tg	140 Tg	61%	11%	15%	10.6
South Asia	6°–33°N, 65°–93°E	1.1 TgN	53 Tg	76 Tg	56%	17%	14%	19.5

[31] Local sources over Japan, which show a strong diurnal variation largely due to boundary layer venting, and regional east Asian sources contribute about 15% and 8%, respectively to O_3 at this site. Regional sources make a larger contribution than local sources during westerly or southwesterly flow that brings high levels of O_3 from China and Korea. European and North American sources each contribute about 3% to O_3 (2–2.5 ppbv), with the smallest contributions (1–1.5 ppbv) during outflow from east Asia. The contribution of stratospheric O_3 largely offsets that from east Asian sources, as flow from these sources is greatest in the warm sector of cyclonic systems or in low-level outflow immediately following the cold front [*Carmichael et al.*, 1998] where the influence of the stratosphere is smallest. Descent of stratospheric air is strongest in the anticyclones separating these systems. The influence of European and North American sources is also greatest in this subsiding air, and there is a good correlation between these sources and stratospheric influence, $r^2 = 0.88$ for North American sources and $r^2 = 0.46$ for European sources. The better correlation for North American sources reflects the higher altitude of transport and hence more similar transport pathway. Note that European and North American fossil fuel sources each have about 20% of the impact on boundary layer O_3 of stratospheric influx at this site. European and North American sources contribute 10% and 8% of CO in April, respectively, a substantial background enhancement, but less than that from other parts of east Asia (16%) or from local sources. Episodes of high CO at Happo coincide with flow from east Asia, when European and North American influences are smallest.

[32] We conclude that transport over Eurasia leads to substantial surface enhancements in long-lived primary pollutants such as CO over Japan, and small but significant enhancements in O_3. These "background" impacts persist during the stagnant, anticyclonic conditions that favor O_3 formation from local sources, and may thus influence the attainment of air quality standards. The 1-hour O_3 standard in Japan, 60 ppbv, is exceeded regularly in springtime, and the enhancements from European and North American sources are likely to contribute significantly to this exceedance.

5.3. Background Ozone

[33] Comparison of surface O_3 measurements at Mondy and Happo with those at Mace Head and Arosa suggests that continental "background" concentrations of O_3, reflecting sources outside the local region, may be larger over northeast Asia than over Europe [*Pochanart et al.*, 2001, 2003a]. Removing precursor emissions from fossil fuel sources over each region independently, we find that boundary layer O_3 over Japan is about 5 ppbv higher than over Europe in autumn and winter and about 10 ppbv higher in March and April. Ab % of this difference is due to higher stratospheric influence associated with descent around the Siberian High or cyclogenesis over east Asia, while the remainder reflects emission sources over Eurasia or stronger descent from the free troposphere. In the summer the difference is reversed, with summertime monsoonal flow from the tropical western Pacific bringing air with O_3 levels 5–10 ppbv lower than those arriving in Europe. While the differences are smaller when evaluated over subcontinental-scale regions than at these selected measurement sites, suggesting that they are not entirely representative of the larger-scale regions, the same patterns can be clearly seen. It is thus clear that precursor sources over northeast Asia build on higher background levels of O_3 than are present over Europe, particularly in spring when O_3 over the region is at a maximum.

6. Global Impacts

[34] We conclude by examining the global impacts of European emissions, and how transport over Eurasia affects them. While the short-term impacts of fossil fuel emissions on air quality over intercontinental distances may be driven principally by changes in O_3, longer-term changes influencing climate are also affected by changes in the OH radical distribution which alter the abundance of long-lived greenhouse gases such as CH_4, HFCs and HCFCs. The impacts on OH are known to be sensitive to the latitude of the source region [e.g., *Gupta et al.*, 1998].

[35] Ozone production from surface sources occurs principally in the boundary layer and lower troposphere, see Table 2. The production efficiency per molecule of NO_x oxidized is lower for sources over Europe than over Asia, where lower NO_x emission intensities, greater insolation at more southerly latitudes and more efficient lifting lead to greater production. The chemical lifetime of O_3 is shorter in the boundary layer, where more than two thirds of gross production from European sources occurs, although this is balanced against outflow at higher latitudes where lower insolation favors longer lifetimes, and consequently the annual mean lifetime of O_3 from European sources is only marginally less than that from North American or Asian sources, see Table 3. The dominance of boundary layer outflow over the continent suggests that deposition may be a more important loss route for O_3 from European sources than from North American and Asian sources, where outflow occurs over the oceans. However, we find only marginally greater deposition, 17% of the gross annual O_3 production versus 14–15% from these other sources. Outflow to the Arctic, Mediterranean and North Africa, where deposition over ice, water or desert surfaces is slow, together with control of surface O_3 by subsidence from the free troposphere at longer timescales may account for this.

Table 3. Annual Mean Tropospheric Chemical Lifetimes

Source Region	CO	O_3
Europe	83 days	18 days
North America	61 days	19 days
East Asia	62 days	21 days
South Asia	56 days	25 days
Tropospheric Mean	55 days	30 days

[36] The more northerly location of outflow from Europe also leads to slower chemical removal of CO, as insolation and OH concentrations are lower, and we thus find that the mean chemical lifetime, 83 days, is longer than from other sources, in agreement with previous studies [*Bey et al.*, 2001]. Tropospheric OH is enhanced by O_3 produced over emission regions but is reduced over more distant regions, where removal by longer-lived CO and hydrocarbons dominates formation from additional O_3. We find that European sources cause a net reduction in annual global mean OH, in contrast to Asian and North American sources which cause an increase, see Figure 14. Changes in radiative forcing due to O_3 from European sources are thus supplemented by changes to long-lived greenhouse gases rather than partially offset by them as from the other regions. Recent reductions in European emissions of NO_x and CO may thus benefit climate through reductions in both O_3 and other longer-lived greenhouse gases. However, a more detailed assessment of the climate impacts of emission changes would need to take into account the seasonal and spatial variations in changes to O_3 and CH_4. The 2-year model runs performed here are too short to determine the long-term changes to CH_4, which has a response time of about 12 years. Nevertheless, this study highlights the sensitivity of climate effects from NO_x and CO emissions to location, as found in previous studies [*Fuglestvedt et al.*, 1999; *Wild et al.*, 2001], and suggests that the impact of these regions on the oxidizing capacity of the troposphere may be significantly different.

7. Conclusions

[37] Europe is a net source of O_3 throughout the year, despite regional depletion caused by NO emissions in wintertime. The regional enhancements or depletion in O_3 are propagated over Eurasia, and lead to increased surface O_3 throughout the Northern Hemisphere except over parts of the Arctic in wintertime, where production and mixing may be insufficient to balance the O_3 reduction transported from Europe. Export of O_3 and its precursors occurs principally in the boundary layer, where lifetimes to chemical removal and deposition are short; however, much of the export occurs at higher latitudes where chemical lifetimes are longer, offsetting this. Enhancements in O_3 are governed principally by transport south or southeastward from Europe and by convective lifting of O_3 and precursors into the free troposphere where one third of gross production may occur.

[38] Over Eurasia we find significant impacts from European sources at 100°E, with the largest enhancements in the boundary layer for CO and in the midtroposphere for O_3. Surface enhancements are generally larger at higher latitudes, with 10–50 ppbv CO in the Arctic, 10–30 ppbv at Mondy and 5–15 ppbv at Mount Waliguan. Enhancements in O_3 may be negative in the Arctic boundary layer in wintertime, but average 4–5 ppbv in spring and summer in midlevel outflow, and reach about 3.5 ppbv at Mondy in spring. The higher altitude of enhancements in O_3 compared to those in CO emphasizes the much shorter boundary layer lifetimes to loss and deposition, and the importance of continued production following lifting into the free troposphere. Over east Asia, European impacts are weaker, 2–25 ppbv for CO and 0.2–2.5 ppbv for O_3 at the surface over Japan. Impacts on O_3 in the midtroposphere are typically smaller and occur at lower altitudes than those from North America, and we demonstrate that this is due to less favorable photochemical and meteorological conditions for boundary layer O_3 buildup over the source region and to weaker lifting processes that carry a smaller proportion into the free troposphere. European and North American contributions to surface O_3 and CO over Japan are largest in spring when they each account for about 3% of O_3 and 10% of CO. While the impacts on O_3 are small, typically 2–2.5 ppbv, they persist during the anticyclonic conditions favoring regional pollutant build up, and thus contribute to reduced air quality over Japan.

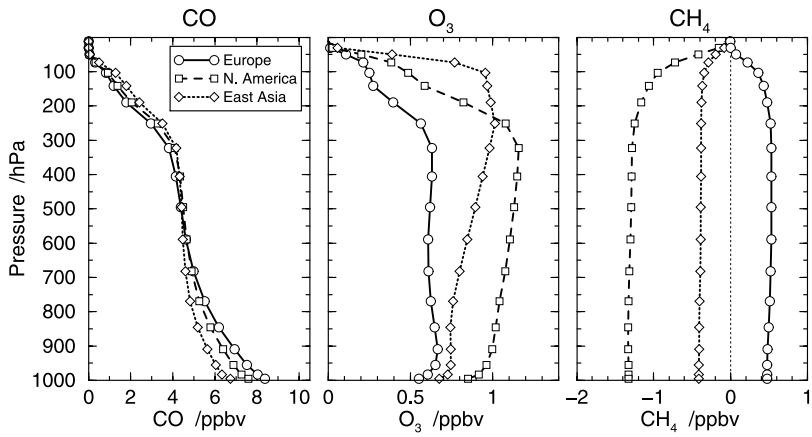

Figure 14. Global annual mean profiles of changes in CO, O_3, and CH_4 due to fossil fuel emissions over industrial regions. These regions account for about 20% of global CO emissions and 40% of NO_x emissions. See version of this figure in the HTML.

[39] European sources have a smaller impact on global O_3 than North American or Asian sources, but have a larger impact on global CO because of slower removal at higher latitudes. We find that they cause a mean net reduction in tropospheric OH, and hence an increase in the lifetime of greenhouse gases such as CH_4, in contrast to the other source regions where OH formation from additional O_3 exceeds greater OH removal. While this suggests differing effects on tropospheric oxidizing capacity, the implications for climate require further study.

[40] This study has been exploratory in nature, and further measurement campaigns and model analysis will be required to identify how the key processes in oxidant formation and transport interact at finer temporal and spatial scales than considered here. While similar results are found with two different sets of meteorological data, we note that substantial uncertainties remain in the sensitivity of O_3 production to convection and deposition processes and in the chemical and radiative effects of coemitted aerosol particles.

[41] In addition to continuation of long-term surface measurements over European and east Asian source regions, we highlight the importance of new observational studies over Eurasia to characterize the evolution of oxidants over the continent. Two regions of particular interest are western Asia, relatively close to European source regions where substantial outflow and lifting occur, and northern Siberia, where much of the boundary layer outflow in springtime occurs inside the Arctic Circle. Measurements at these locations would provide a better insight into the impacts of European sources.

[42] **Acknowledgments.** The authors are grateful to Jostein Sundet for providing the pieced-forecast meteorological fields from the ECMWF Integrated Forecast System and to Manish Naja for helpful discussions.

References

Barrie, L. A. (1986), Arctic air pollution: An overview of current knowledge, *Atmos. Environ.*, *20*, 643–663.

Berntsen, T. J., I. S. A. Isaksen, W.-C. Wang, and X.-Z. Liang (1996), Impacts of increased anthropogenic emissions in Asia on tropospheric ozone and climate, *Tellus, Ser. B*, *48*, 13–32.

Berntsen, T. J., S. Karlsdóttir, and D. A. Jaffe (1999), Influence of Asian emissions on the composition of air reaching the North Western United States, *Geophys. Res. Lett.*, *26*, 2171–2174.

Bey, I., D. J. Jacob, J. A. Logan, and R. M. Yantosca (2001), Asian chemical outflow to the Pacific: Origins, pathways and budgets, *J. Geophys. Res.*, *106*, 23,097–23,114.

Bian, H., M. J. Prather, and T. Takemura (2003), Tropospheric aerosol impacts on trace gas budgets through photolysis, *J. Geophys. Res.*, *108*(D8), 4242, doi:10.1029/2002JD002743.

Cahoon, D. R., Jr., B. J. Stocks, J. S. Levine, W. R. Cofer III, and J. M. Pierson (1994), Satellite analysis of the severe 1987 forest fires in northern China and southeastern Siberia, *J. Geophys. Res.*, *99*, 18,627–18,638.

Carmichael, G. R., I. Uno, M. J. Phadnis, Y. Zhang, and Y. Sunwoo (1998), Tropospheric ozone production and transport in the springtime in east Asia, *J. Geophys. Res.*, *103*, 10,649–10,671.

Cooper, O. R., J. L. Moody, D. D. Parrish, M. Trainer, T. B. Ryerson, J. S. Holloway, G. Hübler, F. C. Fehsenfeld, and M. J. Evans (2002), Trace gas composition of midlatitude cyclones over the western North Atlantic Ocean: A conceptual model, *J. Geophys. Res.*, *107*(D7), 4056, doi:10.1029/2001JD000901.

Derwent, R. G., P. G. Simmonds, and W. J. Collins (1994), Ozone and carbon monoxide measurements at a remote maritime location, Mace Head, Ireland, from 1990 to 1992, *Atmos. Environ.*, *28*, 2623–2637.

Derwent, R. G., P. G. Simmonds, S. Seuring, and C. Dimmer (1998), Observation and interpretation of the seasonal cycles in the surface concentrations of ozone and carbon monoxide at Mace Head, Ireland from 1990 to 1994, *Atmos. Environ. 32*, 145–157.

Duncan, B. N., and I. Bey (2004), A modeling study of the export pathways of pollution from Europe: Seasonal and interannual variations (1987–1997), *J. Geophys. Res.*, *109*, D08301, doi:10.1029/2003JD004079.

Fehsenfeld, F. C., M. Trainer, D. D. Parish, A. Volz-Thomas, and S. Penkett (1996), North Atlantic Regional Experiment 1993 summer intensive: Foreword, *J. Geophys. Res.*, *101*, 28,869–28,875.

Fuglestvedt, J. S., T. K. Berntsen, I. S. A. Isaksen, H. Mao, X.-Z. Liang, and W.-C. Wang (1999), Climatic forcing of nitrogen oxides through changes in tropospheric ozone and methane: Global 3-D model studies, *Atmos. Environ.*, *33*, 961–977.

Graul, R., K. Uhse, and L. Ries (2003), Atmospheric CO and O_3 daily mean measurements at Zugspitze, http://gaw.kishou.go.jp/wdcgg.html, World Data Cent. for Greenhouse Gases, Tokyo.

Gupta, M. L., R. J. Cicerone, and S. Elliott (1998), Perturbation to global tropospheric oxidizing capacity due to latitudinal redistribution of surface sources of NO_x, CH_4 and CO, *Geophys. Res. Lett.*, *25*, 3931–3934.

Hamelin, B., F. E. Grousset, P. E. Biscaye, A. Zindler, and J. M. Prospero (1989), Lead isotopes in trade wind aerosols at Barbados: The influence of European emissions over the North Atlantic, *J. Geophys. Res.*, *94*, 16,243–16,250.

Hansen, J. E. (Ed.) (2002), *Air Pollution as a Climate Forcing: A Workshop*, NASA Goddard Inst. for Space Stud., New York.

Heald, C. L., et al. (2003), Asian outflow and trans-Pacific transport of carbon monoxide and ozone pollution: An integrated satellite, aircraft, and model perspective, *J. Geophys. Res.*, *108*(D24), 4804, doi:10.1029/2003JD003507.

Hoell, J. M., D. D. Davis, S. C. Liu, R. E. Newell, M. Shipham, H. Akimoto, R. J. McNeal, R. J. Bendura, and J. W. Drewry (1996), Pacific Exploratory Mission-West A (PEM-West A): September–October 1991, *J. Geophys. Res.*, *101*, 1641–1653.

Holloway, T., A. M. Fiore, and M. Galanter-Hastings (2003), Intercontinental transport of air pollution: Will emerging science lead to a new hemispheric treaty?, *Environ. Sci. Technol.*, *37*, 4535–4542.

Husar, R. B., et al. (2001), The Asian dust events of April 1998, *J. Geophys. Res.*, *106*, 18,317–18,330.

Jacob, D. J., J. A. Logan, and P. P. Murti (1999), Effect of rising Asian emissions on surface ozone in the United States, *Geophys. Res. Lett.*, *26*, 2175–2178.

Jacob, D. J., et al. (2003), Transport and Chemical Evolution over the Pacific (TRACE-P) aircraft mission: Design, execution, and first results, *J. Geophys. Res.*, *108*(D20), 9000, doi:10.1029/2002JD003276.

Jaegle, L., et al. (2003), Sources and budgets for CO and O_3 in the northeastern Pacific during the spring of 2001: Results from the PHOBEA-II Experiment, *J. Geophys. Res.*, *108*(D20), 8802, doi:10.1029/2002JD003121.

Jaffe, D., et al. (1999), Transport of Asian air pollution to North America, *Geophys. Res. Lett.*, *26*, 711–714.

Jennings, S. G., T. G. Spain, B. G. Doddridge, H. Maring, B. P. Kelly, and A. D. A. Hansen (1996), Concurrent measurements of black carbon aerosol and carbon monoxide at Mace Head, *J. Geophys. Res.*, *101*, 19,447–19,454.

Jonson, J. E., J. K. Sundet, and L. Tarrasón (2001), Model calculations of present and future levels of ozone precursors with a global and a regional model, *Atmos. Environ.*, *35*, 525–537.

Kritz, M. A., J.-C. Le Roulley, and E. F. Danielsen (1990), The China Clipper: Fast advective transport of radon-rich air from the Asian boundary layer to the upper troposphere near California, *Tellus, Ser. B*, *42*, 46–61.

Lelieveld, J., et al. (2002), Global air pollution crossroads over the Mediterranean, *Science*, *298*, 794–799.

Li, Q., D. J. Jacob, J. A. Logan, I. Bey, R. M. Yantosca, H. Liu, R. V. Martin, A. M. Fiore, B. D. Field, and B. N. Duncan (2001), A tropospheric ozone maximum over the Middle East, *Geophys. Res. Lett.*, *28*, 3235–3238.

Li, Q., et al. (2002), Transatlantic transport of pollution and its effects on surface ozone in Europe and North America, *J. Geophys. Res.*, *107*(D13), 4166, doi:10.1029/2001JD001422.

Liu, H., D. J. Jacob, L. Y. Chan, S. J. Oltmans, I. Bey, R. M. Yantosca, J. M. Harris, B. N. Duncan, and R. V. Martin (2002), Sources of tropospheric ozone along the Asian Pacific Rim: An analysis of ozonesonde observations, *J. Geophys. Res.*, *107*(D21), 4573, doi:10.1029/2001JD002005.

Liu, H., D. J. Jacob, I. Bey, R. M. Yantosca, B. N. Duncan, and G. W. Sachse (2003), Transport pathways for Asian pollution outflow over the Pacific: Interannual and seasonal variations, *J. Geophys. Res.*, *108*(D20), 8786, doi:10.1029/2002JD003102.

Louis, J. F. (1979), A parametric model of vertical eddy fluxes in the atmosphere, *Boundary Layer Meteorol.*, *17*, 187–202.

McLinden, C. A., S. Olsen, B. Hannegan, O. Wild, M. J. Prather, and J. Sundet (2000), Stratospheric ozone in 3-D models: A simple chemistry and the cross-tropopause flux, *J. Geophys. Res.*, *105*, 14,653–14,665.

Memmesheimer, M., A. Ebel, and M. Roemer (1997), Budget calculations for ozone and its precursors: Seasonal and episodic features based on model simulations, *J. Atmos. Chem.*, *28*, 283–317.

Naja, M., H. Akimoto, and J. Staehelin (2003), Ozone in background and photochemically aged air over central Europe: Analysis of long-term ozonesonde data from Hohenpeissenberg and Payerne, *J. Geophys. Res.*, *108*(D2), 4063, doi:10.1029/2002JD002477.

Newell, R. E., and M. J. Evans (2000), Seasonal changes in pollutant transport to the North Pacific: The relative importance of Asian and European sources, *Geophys. Res. Lett.*, *27*, 2509–2512.

Novelli, P. C., and K. A. Masarie (2003), Atmospheric CO measurements at Mt. Waliguan, http://gaw.kishou.go.jp/wdcgg.html, World Data Cent. for Greenhouse Gases, Tokyo.

Olsen, S. C., C. A. McLinden, and M. J. Prather (2001), The stratospheric N_2O-NO_y system: Testing uncertainties in a 3-D framework, *J. Geophys. Res.*, *106*, 28,771–28,784.

Parrish, D. D., et al. (1992), Indications of photochemical histories of Pacific air from measurements of atmospheric trace species at Pt. Arena, California, *J. Geophys. Res.*, *97*, 15,883–15,901.

Pochanart, P., H. Akimoto, S. Maksyutov, and J. Staehelin (2001), Surface ozone at the Swiss Alpine site Arosa: The hemispheric background and the influence of large-scale anthropogenic emissions, *Atmos. Environ.*, *35*, 5553–5566.

Pochanart, P., H. Akimoto, Y. Kajii, V. M. Potemkin, and T. V. Khodzher (2003a), Regional background ozone and carbon monoxide variations in remote Siberia/east Asia, *J. Geophys. Res.*, *108*(D1), 4028, doi:10.1029/2001JD001412.

Pochanart, P., H. Akimoto, Y. Kajii, and P. Sukasem (2003b), Carbon monoxide, regional-scale transport, and biomass burning in tropical continental Southeast Asia: Observations in rural Thailand, *J. Geophys. Res.*, *108*(D17), 4552, doi:10.1029/2002JD003360.

Pochanart, P., S. Kato, T. Katsuno, and H. Akimoto (2004), Eurasian continental background and regionally polluted levels of ozone and CO observed in northeast Asia, *Atmos. Environ.*, *38*, 1325–1336.

Purvis, R. M., et al. (2003), Rapid uplift of nonmethane hydrocarbons in a cold front over central Europe, *J. Geophys. Res.*, *108*(D7), 4224, doi:10.1029/2002JD002521.

Raatz, W. E. (1989), An anticyclonic point of view on low-level tropospheric long-range transport, *Atmos. Environ.*, *23*, 2501–2504.

Röckmann, T., C. A. M. Brenninkmeijer, M. Hahn, and N. F. Elansky (1999), CO mixing and isotope ratios across Russia; trans-Siberian railroad expedition TROICA 3, April 1997, *Chemosphere Global Change Sci.*, *1*, 219–231.

Scheel, H. E., et al. (1997), On the spatial distribution and seasonal variation of lower-troposphere ozone over Europe, *J. Atmos. Chem.*, *28*, 11–28.

Solberg, S., F. Stordal, and Ø. Hov (1997), Tropospheric ozone at high latitudes in clean and polluted air masses: A climatological study, *J. Atmos. Chem.*, *28*, 111–123.

Staudt, A. C., D. J. Jacob, J. A. Logan, D. Bachiochi, T. N. Krishnamurti, and G. W. Sachse (2001), Continental sources, transoceanic transport, and interhemispheric exchange of carbon monoxide over the Pacific, *J. Geophys. Res.*, *106*, 32,571–32,589.

Stohl, A. (2001), A 1-year Lagrangian "climatology" of airstreams in the Northern Hemisphere troposphere and lowermost stratosphere, *J. Geophys. Res.*, *106*, 7263–7279.

Stohl, A., S. Eckhardt, C. Forster, P. James, and N. Spichtinger (2002), On the pathways and timescales of intercontinental air pollution transport, *J. Geophys. Res.*, *107*(D23), 4684, doi:10.1029/2001JD001396.

Sundet, J. (1997), Model studies with a 3-D global CTM using ECMWF data, Ph.D. thesis, Dep. of Geophys., Univ. of Oslo, Norway.

Tanimoto, H., Y. Kajii, J. Hirokawa, H. Akimoto, and N. P. Minko (2000), The atmospheric impact of boreal forest fires in far eastern Siberia on the seasonal variation of carbon monoxide: Observations at Rishiri, a northern remote island in Japan, *Geophys. Res. Lett.*, *27*, 4073–4076.

Tanimoto, H., et al. (2002), Seasonal cycles of ozone and oxidized nitrogen species in northeast Asia: 2. A model analysis of the roles of chemistry and transport, *J. Geophys. Res.*, *107*(D23), 4706, doi:10.1029/2001JD001497.

Wenig, M., N. Spichtinger, A. Stohl, S. Beirle, T. Wagner, B. Jähne, and U. Platt (2003), Intercontinental transport of nitrogen oxide pollution plumes, *Atmos. Chem. Phys.*, *3*, 387–393.

Wild, O., and H. Akimoto (2001), Intercontinental transport of ozone and its precursors in a 3-D global CTM, *J. Geophys. Res.*, *106*, 27,729–27,744.

Wild, O., and M. J. Prather (2000), Excitation of the primary tropospheric chemical mode in a global 3-D model, *J. Geophys. Res.*, *105*, 24,647–24,660.

Wild, O., M. J. Prather, and H. Akimoto (2001), Indirect long-term global radiative cooling from NO_x emissions, *Geophys. Res. Lett.*, *28*, 1719–1722.

Zhang, M., I. Uno, S. Sugata, Z. Wang, D. Byun, and H. Akimoto (2002), Numerical study of boundary layer ozone transport and photochemical production in east Asia in the wintertime, *Geophys. Res. Lett.*, *29*(11), 1545, doi:10.1029/2001GL014368.

H. Akimoto, P. Pochanart, and O. Wild, Frontier Research System for Global Change, 3172-25 Showa-machi, Kanazawa-ku, Yokohama, Kanagawa 236-0001, Japan. (akimoto@jamstec.go.jp; pakpong@jamstec.go.jp; oliver@jamstec.go.jp)

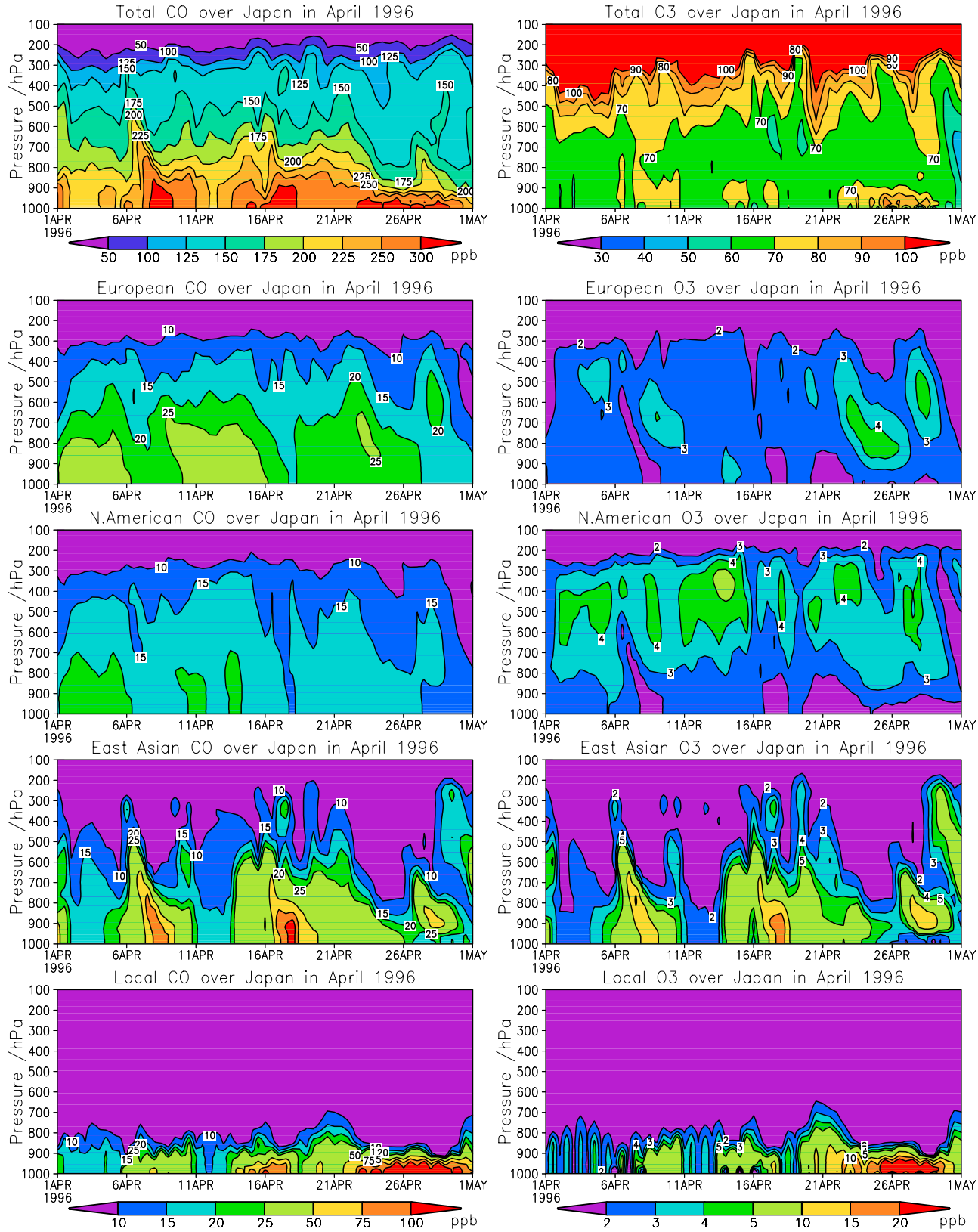

Figure 11. Evolution of the profiles of (left) CO and (right) O_3 over Happo, Japan, in April 1996, together with contributions from European, North American, regional east Asian, and local Japanese fossil fuel sources.